Technical Note

Effect of wearing a face mask on fMRI BOLD contrast

Christine S.W. Law [a],[*], Patricia S. Lan [b],[c], Gary H. Glover [b],[c]

[a] Systems Neuroscience and Pain Lab, Department of Anesthesiology, Perioperative and Pain Medicine, Stanford University School of Medicine, Palo Alto, CA, 94304, USA
[b] Department of Bioengineering, Stanford University, 443 Via Ortega, Stanford, CA, 94305, USA
[c] Department of Radiology, Stanford University, 1201 Welch Road, Stanford, CA, 94305, USA

ARTICLE INFO

ABSTRACT

International spread of the coronavirus SARS-CoV-2 has prompted many MRI scanning facilities to require scan subjects to wear a facial covering ("mask") during scanning as a precaution against transmission of the virus. Because wearing a mask mixes expired air with the subject's inspired air stream, the concentration of inspired carbon dioxide $[CO_2]$ is elevated, resulting in mild hypercapnia. Changes in the inspired gas mixture have been demonstrated to alter R2*-weighted Blood Oxygen Dependent (BOLD) contrast. In this study, we investigate a potential for face masking to alter BOLD contrast during a sensory-motor task designed to activate visual, auditory, and sensorimotor cortices in 8 subjects. We utilize a nasal cannula to supply air to the subject wearing a surgical mask in on-off blocks of 90s to displace expired CO_2, while the subject performs the sensory-motor task. While only a small fraction (2.5%) of the sensory-motor task activation is related to nasal air modulation, a 30.0% change in gray matter BOLD signal baseline is found due to air modulation. Repeating the scan with mask removed produces a small subject-specific bias in BOLD baseline signal from nasal air supply, which may be due to cognitive influence of airflow or cannula-induced hypoxia. Measurements with capnography demonstrate wearing a mask induces an average increase in $ETCO_2$ of 7.4%. Altogether, these results demonstrate that wearing a face mask during gradient-echo fMRI can alter BOLD baseline signal but minimally affects task activation.

1. Introduction

The widespread incidence of infection from the novel coronavirus SARS-CoV-2 has prompted many research MRI scanning facilities to require continuous facial covering (wearing a mask) by scan subjects during scanning in order to diminish the risk of virus transmission, especially since many of those infected are asymptomatic. The purpose is primarily to contain respiratory droplets that can harbor the virus so they avoid landing on surfaces or remain in the air potentially to infect others. There are numerous styles of masks (CDC, 2020), ranging from cloth and surgical procedure masks to N95 respirators, having various degrees to which expired air is retained for one or more respiration cycles. Wearing an efficacious mask will mix some expired air with fresh air, and lead to increased carbon dioxide concentration $[CO_2]$ in inspired air. The question we approached is: Since CO_2 is a potent vasodilator, does this elevation in $[CO_2]$ alter functional MRI (fMRI)?

fMRI is an epiphenomenological indicator of neural activity, relying on changes in blood oxygenation to depict metabolism changes consequent to neuronal modulation, demonstrated in gradient-recalled echo (GRE) imaging as changes in the susceptibility weighted relaxation rate R2*. The resulting Blood Oxygen Level Dependent (BOLD)

contrast (Ogawa et al., 1990) is subject to confounds that can alter the oxygen content independent of neural metabolism including, for example, changes in baseline cerebral blood flow (CBF) (Davis et al., 1998, Kastrup et al., 1999, Buxton and Frank, 1997). Oxygen content of arterial blood is affected by air exchange in the lungs; thus concentrations of oxygen $[O_2]$ and carbon dioxide $[CO_2]$ in inspired air will be represented in blood chemistry delivered to the brain. In particular, breathing air with increased $[CO_2]$ will cause increased arterial blood flow to vascularized brain tissue, mainly in gray matter (Wise et al., 2007).

The purpose of this study is to examine the effect of wearing a mask on BOLD contrast while subjects perform a robust sensory-motor (visual, auditory, sensorimotor) task as the gas content in inspired air is manipulated by periodically supplying fresh air through a nasal cannula. We hypothesize that without a mask, supply of fresh air in the nasal cannula will have minimal effect on air content and cause little change in BOLD contrast due to CO_2 (except for cognitive changes induced by the air flow). On the other hand, any change in BOLD contrast due to fresh air supply while wearing a mask is readily explained by the change in air content (i.e. less CO_2 accumulation during fresh air supply).

We first model the change in BOLD contrast that results from elevated end tidal CO_2 ($ETCO_2$), and then describe fMRI scans to test the

---
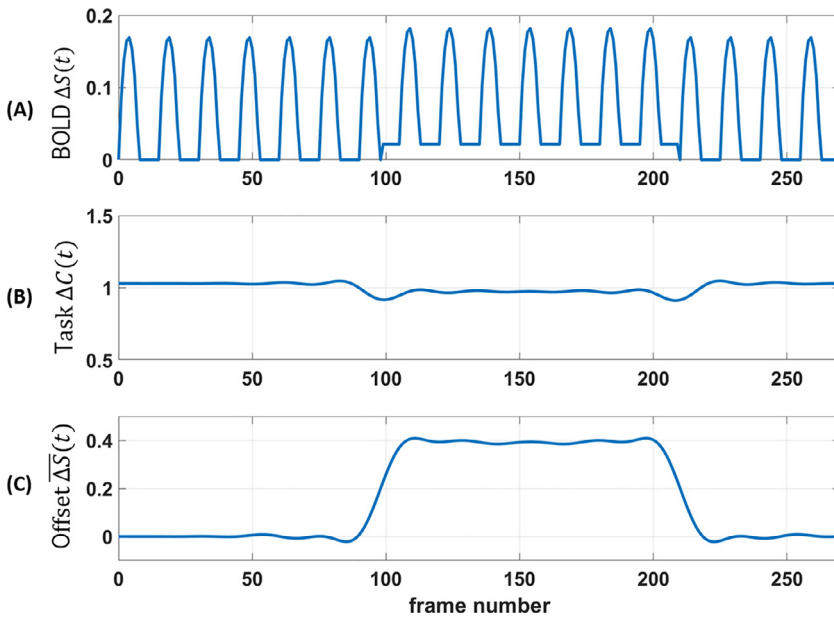
Fig. 1. Simulation. (A) Model of BOLD contrast during task with half-sinusoidal CMRO2 variation, square wave increases in *CBF* during time frames 100-210, A = 0.02. Simulation set maximum BOLD factor M = 1. (B) Sliding window analysis of task contrast (Eq. 4b) does not vary substantially during elevated *CBF* (except artifactually at transitions near frames 100 and 210). (C) Sliding window analysis of modeled task offset (Eq. 4a) demonstrates baseline shift during elevated *CBF*. ΔC and $\overline{\Delta S}$ are normalized by average task contrast.

degree and character of alterations that are observed while wearing a mask. In separate measurements using capnography, we quantify the change in $ETCO_2$ levels induced by wearing a mask.

2. Theory

2.1. Simulation

Hypercapnia causes an increase in BOLD signal (Wise et al., 2007), due to elevated Cerebral Blood Flow (CBF), resulting from the vasodilatory response to increased arterial blood $[CO_2]$. The increase in blood flow causes reduced deoxyhemoglobin concentration and a decrease in R2*. The relationship between BOLD signal (ΔS), Cerebral Metabolic Rate of Oxygen (*CMRO2*), and *CBF* is given in the Davis model (Davis et al., 1998) as a function of time (*t*) by

$$\frac{\Delta S(t)}{\Delta S_0} = M\left\{1 - \left(\frac{CMRO2(t)}{CMRO2_0}\right)^{\beta}\left(\frac{CBF(t)}{CBF_0}\right)^{\alpha-\beta}\right\} \quad (1)$$

where M is the maximum BOLD contrast that can be obtained in the given brain region, $\alpha \sim 0.4$ is Grubb's constant expressing an empirically-derived power law relationship between blood volume and CBF (Grubb et al., 1974), $\beta \sim 1.5$ is a constant relating signal change to concentration of deoxyhemoglobin determined by Davis, et. al, and the subscript 0 represents baseline values. We modeled the task-elicited change in metabolism as

$$\frac{CMRO2(t)}{CMRO2_0} = 1 + cF(t) \quad (2a)$$

where

$$F(t) = \begin{cases} \sin\left(\frac{2\pi t}{T}\right), & \sin\left(\frac{2\pi t}{T}\right) > 0 \\ 0, & \sin\left(\frac{2\pi t}{T}\right) \leq 0 \end{cases} \quad (2b)$$

where c is a constant, and T is the period of the task. Because the task design we used has an intentionally short block duration (15s), the evoked hemodynamic response can be well modeled by a sine wave with frequency $1/T$. $F(t)$ describes only positive increases in metabolism during on blocks.

Total change in $CBF(t)$ comprises the task-elicited change and the change from turning air on:

$$\frac{CBF(t)}{CBF_0} = 1 + dF(t) + A(t) \quad (3)$$

where d is a constant which describes the amplitude of the task-elicited change and $A(t)$ is a square wave representing an additional positive modulation of CBF due to air flow.

This model assumes that modulating $[CO_2]$ by airflow in the mask does not in itself cause BOLD changes from a potential cognitive influence of sensing airflow in the nose. Simulation results are shown in Fig. 1A for $T = 30$ s, 270 time frames, 2 s sampling interval (TR), $A = 0.02$, $d = 0.45$, $c = 0.16$ (Davis et al., 1998). The $[CO_2]$-induced CBF increase occurs during time frames 100 – 210 and leads to an elevated BOLD baseline signal, but only an insignificantly decreased BOLD amplitude.

2.2. Quantification

In order to characterize the effect on BOLD contrast due to air manipulation in the measured BOLD timeseries data, $\Delta S(t)$, a sliding window analysis was performed to test for a baseline shift in the BOLD timeseries as well as for task contrast change. The baseline shift is

$$\overline{\Delta S}(t) = \frac{1}{nT}\int_{t-nT/2}^{t+nT/2} \Delta S(t')dt' \quad (4a)$$

The task design regressor is modeled by a sine wave with frequency $1/T$. Therefore the sliding window task contrast change is approximated as

$$\Delta C(t) = \frac{1}{nT}\int_{t-nT/2}^{t+nT/2} \Delta S(t')\sin\left(\frac{2\pi t'}{T}\right)dt' \quad (4b)$$

By setting window width to an integer multiple of the task period, $\overline{\Delta S}(t)$ is therefore an estimate of slowly varying task signal amplitude. Similarly, changes in $\Delta C(t)$ represent alterations in timeseries signal at the task frequency and can be taken to infer task contrast changes during the scan.

This analysis was applied to a simulated timeseries with window duration $= T$ ($n = 1$). We intentionally chose a small value for CBF change (A = 0.02) to mimic the small hypercapnic effects of wearing a mask. The result is shown in Fig. 1B,C. As predicted, with elevated CBF hypothesized to occur due to increased $ETCO_2$ with mask on and no added fresh air, there is a baseline shift $\overline{\Delta S}(t)$ but not a substantial task contrast change $\Delta C(t)$ in BOLD signal. Note, however, if a subject's breathing rate or mask efficacy changes during the scan, hypercapnia levels could change. Consequent CBF variation would lead to added noise in
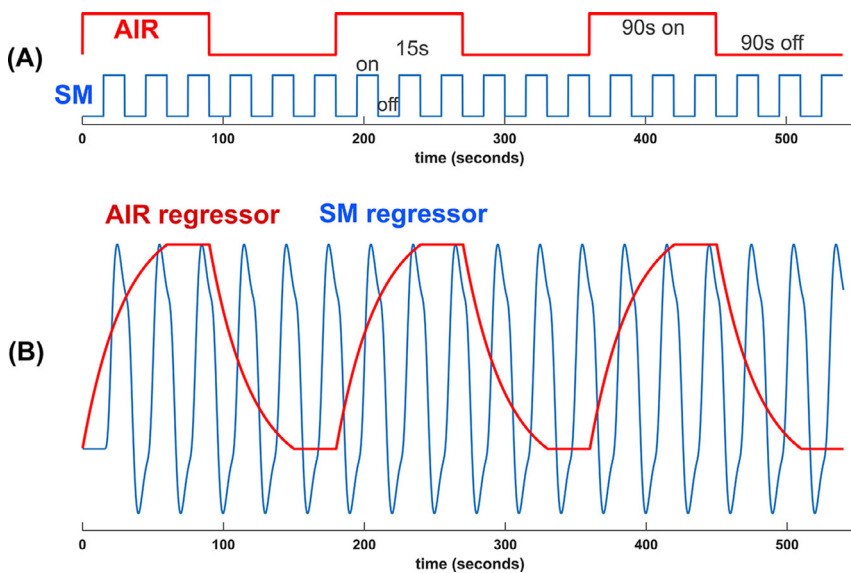
Fig. 2. (A) Sensory-motor (SM) and air-on/off (AIR) task block design. (B) Regressors for SM and AIR. Scan duration is 540s long. Because of the short period of the SM task, its regressor is approximated as a sine wave in subsequent sliding window analyses.

the BOLD signal, which could result in reduced statistical power in predicting task activation.

3. Methods

3.1. Experimental design

We sought to study whether wearing a mask would induce enough hypercapnia from rebreathing expired air to affect BOLD activation in a task. To activate visual, auditory, and sensorimotor regions, we chose a robust block design sensory-sensorimotor (SM) task: the on-block consisting of a contrast-reversing (flashing at 3Hz) checkerboard, synchronously changing tones spanning one octave presented in pseudo-random order, and subject sequentially tapping thumb to four digits on the right hand synchronous in time with the tones and flashing checkerboard. The off-block is a fixation cross. The on and off blocks are intentionally short (15s) so that the BOLD response is well represented by a sine wave at the fundamental task frequency of 1/30Hz. During this task, medical-grade air (air-on/off blocks; AIR) was supplied to the subject through a nasal cannula, in 90s duration on and off blocks (Fig. 2A). The SM and AIR designs are nearly orthogonal to each other (correlation coefficient = 0.013), which allows their characterization using a general linear model (GLM).

A GLM with two design regressors is used to separately generate activation maps of the sensory-motor (SM) task and hypercapnia (AIR) effect. The sensory-motor task regressor is a square wave convolved with hemodynamic response function (Glover, 1999), while the AIR regressor uses an exponential response function (30s time constant suggested during pilot scans) convolved with a square wave (Fig. 2B). The 9 minute-long scan was repeated with mask removed, which was expected to eliminate hypercapnic modulation of BOLD signal.

3.2. Subjects

Eight healthy subjects (3 males, 5 females, age 44 ± 16 years) from Stanford University community were enrolled in the study after giving informed consent for a research protocol approved by the Stanford University IRB. A nasal cannula (Hudson RCI flared, Teleflex Medical, Research Triangle Park, NC) was placed in the subject's nose and tubing cinched comfortably around the back of the head. A pleated surgical procedure mask with the metal nose strip removed (for RF and magnetic safety) was placed over the cannula and face, covering the nose and extending to the chin. With the metal strip removed the mask did

not fit snugly to the face, so surgical tape was used to affix mask to face, attempting to seal the gap. During the "mask-off" scan the mask was slid downward to uncover the nose and mouth. In this mode expired air was not rebreathed because of the flow in the bore from the scanner's bore fan. The subject was able to perform the "mask-off" or "mask-on" maneuver between scans, with minimal head motion. The order of mask-on and mask-off scans was counterbalanced between subjects.

3.3. Breathing apparatus

Air was supplied to the cannula at a rate of 5.8 L/min from a tank of medical-grade air through a regulator and solenoid valve controlled by a computer also presenting the sensory-motor task stimuli with Eprime software (Psychology Software Tools, Sharpsburg, PA). During both "mask-on" and "mask-off" scanning, the airflow was cycled in 90s off-on blocks (AIR) while subjects performed the SM task. The flow rate was sufficient to provide fresh air within the mask approximately equal to the average human breathing rate (Warner and Patel, 2018), displacing expired air.

3.4. fMRI scanning

A 3T MRI scanner with 48-channel head coil (GE Premier, Milwaukee, WI) was employed. The scanner's bore fan was turned on at low. Anatomic scans were acquired with a 3D T1-weighted (BRAVO) sequence with 22cm FOV, 192×256 matrix, 32 4-mm thick slices, in axial plane. Functional scans employed a gradient echo $R2^*$-weighted spiral-in/out pulse sequence (Glover and Law, 2001) with the same slice prescription as the anatomic scan, 64×64 matrix, TR/TE 2000/30 ms, 77° flip angle, 270 time frames (9 minute scan duration). Physiological data were acquired with the scanner's respiration belt on the upper abdomen and pulse oximeter on the subject's left index finger. Pneumatic earphones and padding stabilized the head to diminish head motion. No-mask fMRI data were not obtained for subject #8 (Table 1) due to technical failure and inability to repeat the scan.

3.5. Activation maps

Postprocessing of timeseries images was performed with conventional, homemade software, which included 6-parameter motion correction, correction of cardiac and respiration confounds using RETROICOR (Glover et al., 2000) and RVHRCOR (Chang et al., 2009), and spatial smoothing with a 1.5 pixel FWHM 3D Gaussian kernel. RETROICOR

Table 1
Sliding window timeseries analyses.

Subject	Fractional task contrast change ΔC_f		Fractional baseline shift ΔS_f		Total RMS motion (mm)	
	With Mask	No Mask	With Mask	No Mask	With Mask	No Mask
1	0.012	0.040	0.130	0.752	0.14	0.19
2	0.013	0.086	-0.028	0.110	0.18	0.12
3	-0.017	-0.034	0.032	-0.169	0.13	0.10
4	-0.024	0.033	0.103	0.119	0.12	0.11
5	0.134	0.082	1.726	0.042	0.18	0.14
6	0.078	-0.037	0.366	-0.381	0.12	0.17
7	0.000	-0.030	0.000	-0.017	0.27	0.16
8	0.006	—	0.071	—	0.20	—
Average	0.025	0.020	0.300	0.065	0.17	0.14

Table 1: Fractional change in task contrast ΔC_f and baseline shift ΔS_f for each subject. The AIR-related average task contrast changes with or without mask (2.5%, 2.0%, respectively) were not significant while the average baseline signal shift with mask-on (30.0%) was significant. The average baseline signal shift of 6.5% (without mask) was not significant. No data were obtained on subject #8 without mask due to technical failure. No significant difference in subject motion is noted between scans with and without mask.

and RVHRCOR were not applied to subject #7 whose physiological data were heavily correlated with the SM task. The GLM analysis used quadratic detrending together with design regressors shown in Fig. 2B. For generating group activation maps, FSL v6.0 software (Jenkinson et al., 2012) was used to normalize activation maps to a common MNI atlas.

3.6. Analysis

Timeseries were extracted from each scan using an ROI consisting of those voxels with sensory-motor task activation T-scores exceeding 5.0, (i.e, uncorrected p-values of 5e-7). The resulting timeseries was submitted to the sliding window analysis in Eq. 4(a,b) for scans with and without mask for each subject.

To quantify the degree to which the time varying task contrast $\Delta C(t)$ and baseline shift $\overline{\Delta S(t)}$ were affected by the airflow modulation, covariation of these signals with the AIR regressor (shown in Fig. 2B) were calculated for each subject's mask-on and mask-off data. The results were expressed as fractional changes with integrations covered the scan duration:

$$\Delta S_f = \frac{\int \overline{\Delta S}(t) \, AIR(t) \, dt}{mean(\Delta C(t)) \int AIR(t) \, dt} \tag{5a}$$

$$\Delta C_f = \frac{\int \Delta C(t) \, AIR(t) \, dt}{mean(\Delta C(t)) \int AIR(t) \, dt} \tag{5b}$$

3.7. Subject motion

Subject motion was estimated by calculating the brain centroid of each volume before removing baseline drift or motion correction. Root-mean-square (RMS) values of motion in x, y, and z dimensions were computed. Total RMS motion is the square root of sum of squares of RMS motions in x, y, and z.

3.8. ETCO$_2$ measurement

End tidal CO_2 measurements were made in separate sessions with subjects outside the scanner, employing the identical or same type of mask and cannula as utilized during scanning. The cannula was connected to a patient monitor (Medrad Veris 8600, JZ Imaging, Willoughby, OH) employing infrared gas capnography. Readings were obtained every 15s for 5 min with mask in place as during scanning, and with the mask removed. Two to three minutes of stabilization time

was employed before and between measurement blocks. The normalized difference between mask-on and mask-off ETCO$_2$ was computed as

$$\Delta ETCO_2 = \left(\overline{ETCO_{2on}} - \overline{ETCO_{2off}} \right) / \overline{ETCO_{2off}} \tag{6}$$

where $\overline{ETCO_{2on,off}}$ denote the 5-minute-average readings with and without the mask, respectively. A heteroscedastic T-test was employed to determine the significance of the $\Delta ETCO_2$ in each subject, and a paired T-test was employed to test the overall significance across the cohort. To examine the possibility that breathing conditions could be different in the magnet from the bore fan and confinement, the measurements were repeated with subject #7 in the magnet performing the SM task (but without scanning).
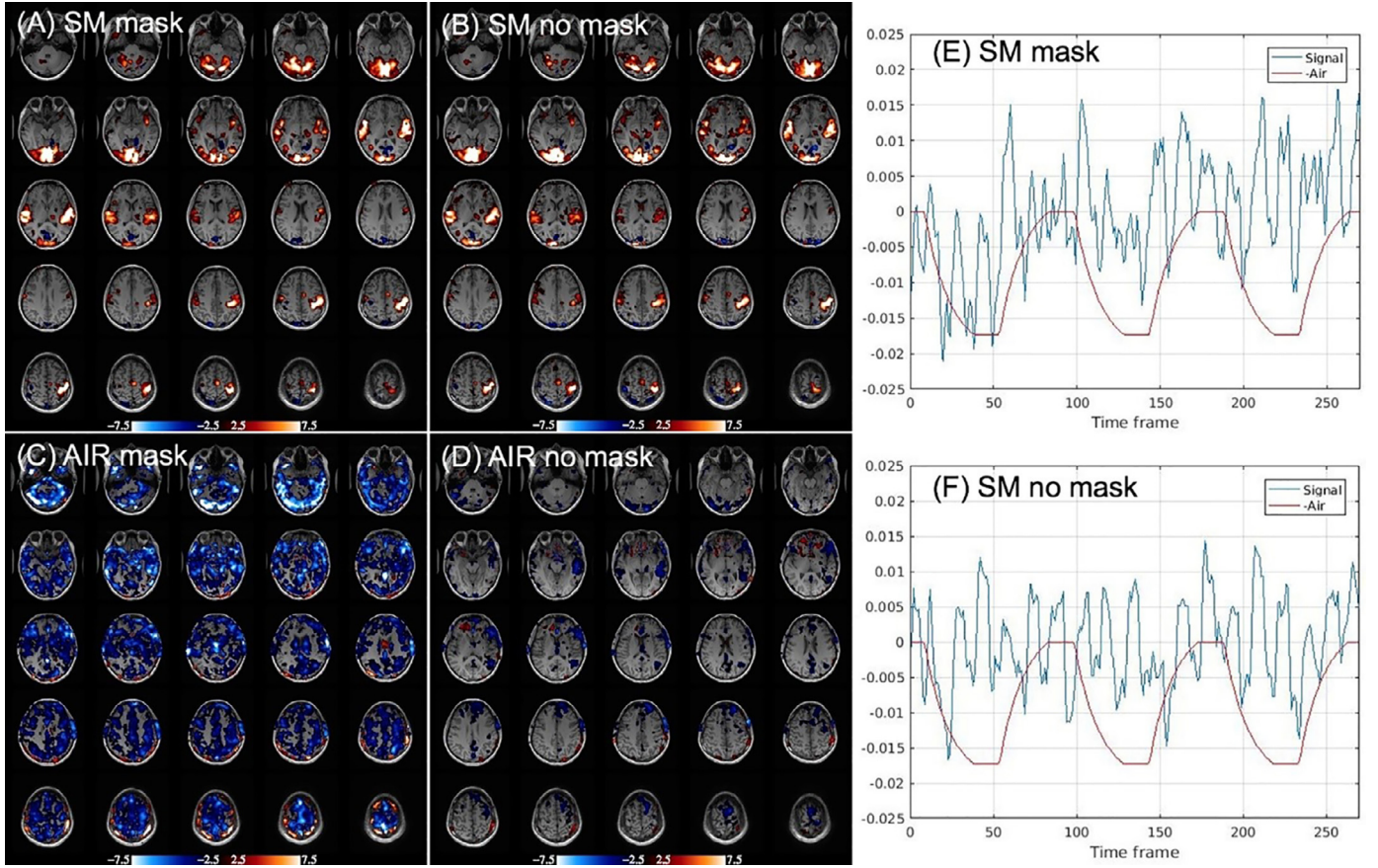
4. Results

4.1. Task activation

Fig. 3 shows single-subject activation results for the sensory-motor task and for air-on/off blocks, each with and without mask. Task activation in Fig. 3A,B focused in visual, auditory, and sensorimotor cortices, remains robust with or without mask. The difference between mask and no mask task activation (maps not shown) is not significant. Supplying air while wearing mask (Fig. 3C) reduces mask-induced hypercapnia, resulting in widespread deactivation of BOLD signal predominantly in gray matter, as expected. When the mask is removed (Fig. 3D), BOLD signal related to air-on/off blocks demonstrates marked reduction, as expected with normoxia. Deactivation was observed for the mask-off condition in some individual subjects; for example, insula cortex and frontal region in Fig. 3D. This suggests a cognitive influence derived from sensation of airflow induced by the nasal cannula. With mask on, some subjects reported a sense of nasal airflow. Some cognitive effect of sensing nasal cannula airflow could be retained with the mask off. Fig. 3E,F blue plots show timeseries of highly activated voxels, obtained by averaging all voxels with SM activation having T scores > 5.0 (uncorrected p-value 5E-7), from scans shown in Fig. 3A,B. Also shown is the AIR regressor, inverted to demonstrate that baseline signal is elevated during air off periods with mask (Fig. 3E) but correlates negligibly with AIR without mask (Fig. 3F).

The timeseries for each subject (as calculated for subject #3 in Fig. 3E,F) was submitted to the sliding window analysis in Eq. 4(a,b). Fig. 4 shows the result of averaging these sliding-window timeseries across subjects to obtain the effect of air-on cycles on task contrast change ΔC and baseline signal offset $\overline{\Delta S(t)}$.

Table 1 provides a summary of the sliding window analysis for each subject presented as fractional changes in SM task contrast ΔC_f and
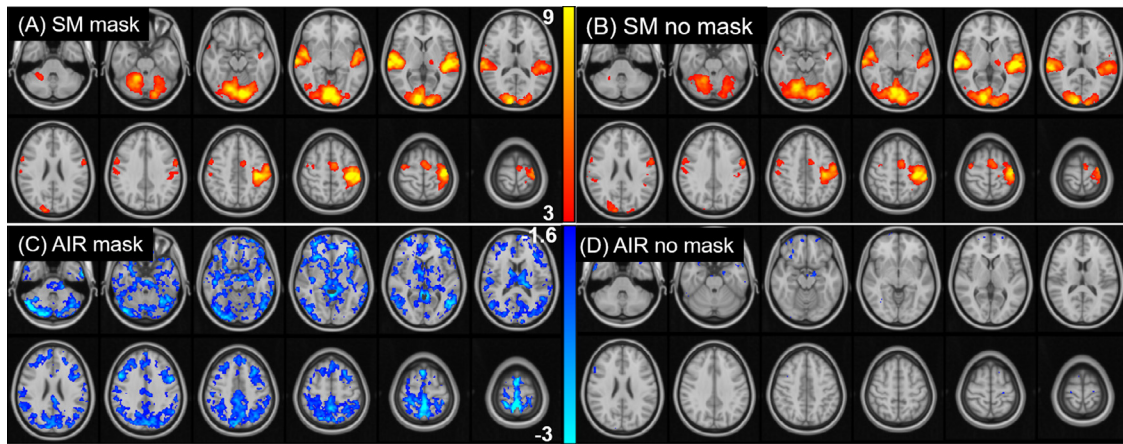
Fig. 3. Single-subject (#3 in Table 1) activation results. (A), (B): Sensory-motor (SM) task (task > fixation). (C), (D): AIR effect (air-on > air-off). Color bars reflect T-scores (red > 0, blue < 0). Deactivation in (C) demonstrates the baseline signal is larger with air-off due to mask-induced mild hypercapnia. (D) Without mask, there is negligible global gray matter deactivation but some subjects exhibit cognitive deactivation due to sensing airflow. (E) Timeseries plot of activated voxels (percentage change, T > 5.0, blue) from scan with mask (A), together with AIR regressor (red), which is plotted negatively to confirm signal is elevated during air off. (F) Timeseries plot of same voxels with no mask scan in (B).
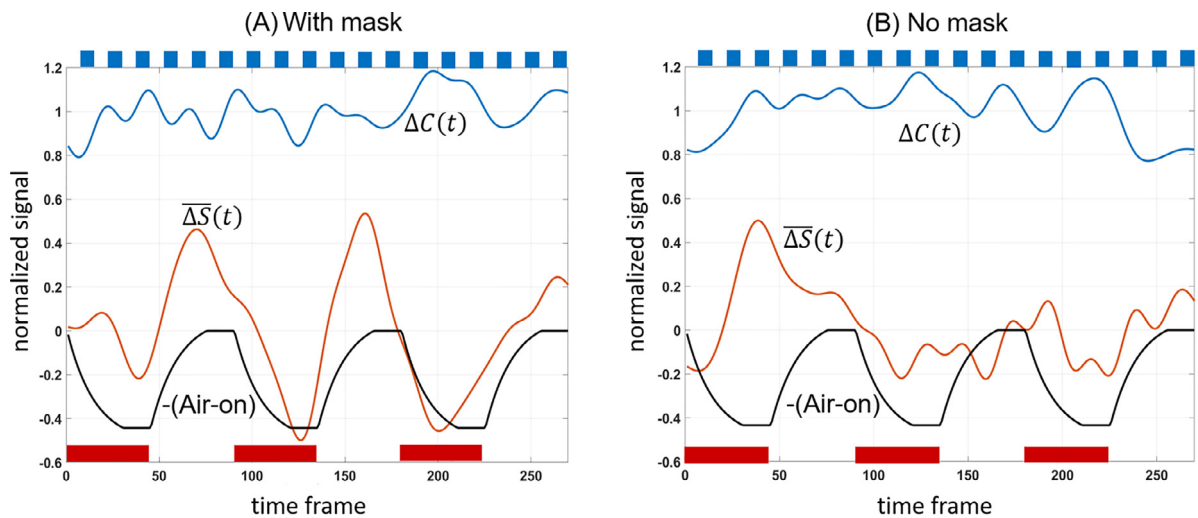
Fig. 4. Subject-averaged sliding window plots showing task contrast amplitude $\Delta C(t)$, baseline signal offset $\overline{\Delta S}(t)$, and AIR regressor (with sign reversed to demonstrate its anticorrelation with $\overline{\Delta S}$). Red bars on the figure represent Air-on periods while top blue bars represent SM task on-blocks. Signal was normalized by the mean of task contrast for each subject before averaging.

Fig. 5. Group activation results: (A)(B) Sensory-motor (SM) task (task > fixation). No significant group-level difference in SM task with and without wearing masks. (C)(D) AIR effect (air-on > air-off). Global gray matter deactivation observed due to wearing masks (C) is not detected when masks were removed (D). Color bars reflect T-scores. Mask results were averaged from 8 subjects while No Mask results were averaged from 7 subjects.

Table 2
End tidal CO2 measurements.

Subject	ETCO$_2$, mm Hg		ΔETCO$_2$ (p value)
	With mask	No mask	
1	36.8	33.1	0.111 (2E-14)
2	42.6	36.8	0.157 (3E-14)
3	36.2	33.7	0.074 (5E-14)
4	35.6	32.9	0.080 (6E-06)
5	41.2	39.2	0.050 (1E-06)
6	31.2	30.6	0.021 (0.036)
7	36.0	33.7	0.066 (2E-08)
	31.4*	29.5*	0.063* (2E-05*)
8	33.5	32.5	0.032 (5E-03)
Average	—	—	0.074

Table 2: ETCO$_2$ measurements with and without surgical mask. Normalized fractional difference (ΔETCO$_2$) was calculated from Eq.6. Subject #7* capnography data were collected in the scanner performing the SM task but not being scanned.

fractional changes in baseline shift ΔS_f calculated by covariation with the AIR regressor (Eq. 5a,b) as well as subjects head motion information. With mask on, the average baseline shift was 30.0% ($p < 0.0141$) while the average task contrast change was not significant (2.50%, $p = 0.43$) from covariation with AIR. With mask removed, there was no significant covariation of task contrast (2.0%, $p = 0.45$) or baseline shift (6.5%, $p = 0.21$) with AIR. Subject motion was small in this cohort of motivated volunteers, and not correlated with the AIR blocks. Paired-sample T-test shows no significant difference in motion with and without mask.

Sensory-motor task and air-on/off responses for single-subject maps in Fig. 3 are as robust as responses averaged across subjects in Fig. 5. Sensory-motor task activation can be detected reliably under both mask-on and mask-off conditions (Fig. 5A,B) with no significant activation difference between conditions. Global gray matter deactivation is seen under mask-on and lack of airflow (Fig. 5C). Comparing to the entire gray matter volume, the amount of deactivation (due to mild hypercapnic or cognitive effects from airflow) is insignificant without mask at group level (Fig. 5D).

4.2. ETCO$_2$ Measurements

Table 2 shows ETCO$_2$ measurements on subjects outside the magnet, as well as results on subject #7 in the magnet performing SM task but without scanning. The average change in ETCO$_2$ was 7.4% increase when wearing a mask. A paired T-test across subjects confirmed that this difference is significant at $p < 0.0014$. Our measurement of ETCO$_2$ increase from wearing a surgical mask is similar to that when wearing N-95 masks (Bharatendu et al., 2020).

5. Discussion and Conclusion

The experiments in this study employed a nasal cannula to replace expired air with fresh air in a block design, thereby allowing controlled manipulation of endogenous [CO$_2$] levels during a sensory-motor task in two separate scans (one with mask and one without mask). The results, while wearing a mask, demonstrated good qualitative agreement with the model; showing no significant change in task activation ($p = 0.43$) but significant change in baseline signal compared to the condition when fresh air was introduced into nasal passages ($p < 0.0141$). These results confirm that wearing a mask increases the BOLD baseline signal (30% on average, Table 1) through reduced R2*, but the effect does not substantively alter gain of task-induced changes in signal; i.e, estimates of task activation with and without mask (Table 1). Results with no mask demonstrated negligible alteration to task activation, although some subjects showed localized baseline signal shift correlated with air-on (Fig. 3D). This result was unexpected because there should not be a hypercapnic change with mask removed and air flowing. We speculate that such a baseline shift could be due to cognitive effects of airflow sensation or a result of mild hypocapnia from fresh air being introduced in the nose. Nevertheless, Figs 3D and 5D illustrate that hypercapnic effect is largely absent with mask removed, as expected.

The measurements of end tidal CO$_2$ were made outside the scanner, as quantitation was not possible while scanning and modulating the air using a cannula, because of mixing of the delivered air with the sampled expired air. Using a gas mask with rebreathing valve instead of nasal cannula would prevent the mixing effect and allow ETCO$_2$ measurement while delivering air, but the substantial complexity would violate the concept of simply wearing a facial covering during fMRI. Results showed that reliable mild hypercapnia was induced with mask on (average 7.4% increase in ETCO$_2$ relative to no-mask condition). Differences with and without mask were significant within subjects (shown in Table 2) and in the cohort ($p < 0.0014$, paired T-test). However, to suggest that changes in ETCO$_2$ measured in the control room were similar to those during scanning, the measurements were repeated in the scanner (without fMRI but performing the SM task) on one subject. The capnography measurement on subject #7 inside and outside the scanner were comparable as shown in Table 2.

While there were individual differences in BOLD signal amplitude and ETCO$_2$ across subjects, we estimated the average BOLD reactivity to $\Delta ETCO_2$. For each subject, we calculated an individual AIR-activation gray matter mask (mask-on data correlated with AIR regressor having Z-score > 4 within gray matter). Each subject's BOLD signal data was filtered by their masks to calculate percent signal change. Averaging each individual's percent signal change per mmHg gave an estimate of BOLD reactivity to $\Delta ETCO_2$ of 0.36%/mmHg. This value is slightly less than that observed in gray matter by Prisman, et al. (Prisman et al., 2008) (0.44%/mmHg) in 4 participants during controlled hypercapnia. The difference may be due to lack of precision control of the mask and cannula in our study. However, with limited number of subjects in both studies, quantitation is underpowered.

While wearing a facial covering during fMRI does not substantially alter task activation, it may create sensitivity to changes in respiration or mask placement through variations in inspired [CO$_2$] that are absent without a mask. Some subjects may have experienced facial discomfort, for example, prompting adjustments of their mask during scan. This effect would manifest as a difference between sliding-window timeseries noise levels with and without mask. In the present study, no significant differences were found in the task contrast change $\Delta C(t)$ between scans with and without mask (Table 1), suggesting that wearing a mask contributes a negligible effect to BOLD activation in our sensory-motor experiments.

Our study is subject to a number of limitations: Only a small cohort (8 subjects) could be recruited from within our lab because of institutional regulations prompted by the pandemic. Of these, only 7 no-mask scans were obtained for technical reasons. Only one type of mask was evaluated. Different respirators may confine expired air more tightly and exacerbate baseline signal change, although our results were similar to observations made with N-95 masks (Bharatendu et al., 2020). Only a robust sensory-motor task was evaluated, although effects on verbal working memory were anecdotally tested and found to be congruent with the SM results. In addition, we gathered three resting-state data sets and analyzed the connectivity in the default mode network. Although our initial results in functional connectivity, ALFF, FALFF, and global signal show no significant effect from wearing a mask, a substantially larger sample size would be needed to reliably detect small resting state signal changes.

Because of recruitment limitations on the size of our subject cohort, we used block-design air manipulations in an attempt to more robustly estimate mask effects within a single scan than calculating differences between separate scans with different airflow. In preliminary studies, several subjects wearing a mask performed SM during separate scans, twice each with and without continuous air supply (4 scans total). We found that in the two repetitions without changing the air flow condition, the SM task amplitude was not reproducible enough to make reliable estimates of the difference of adding air to the cannula. Poor reproducibility between scans, could presumably due to variations in task performance, vigilance, and habituation, is consistent with earlier studies of fMRI reproducibility (Voyvodic, 2006).

In summary, wearing a mask increases ETCO$_2$ by 7.4% measured by gas capnography. Increased [CO$_2$] causes increased CBF and reduced R2*, and induces global gray matter activation changes as in a CO$_2$ gas challenge (Wise et al., 2007) or breath holding (Kastrup et al., 1999). This hypercapnic effect causes a change in signal baseline level but no significant change in task activation.

Data availability

Data reported in this manuscript can be made available with permission from Stanford University.

Credit author statement

Christine S W Law: Conceptualization, Methodology, Formal analysis, Investigation, Writing – Review & Editing, Visualization

Patricia S Lan: Conceptualization, Methodology, Investigation, Writing – Review & Editing

Gary H Glover: Conceptualization, Methodology, Formal analysis, Investigation, Writing – Review & Editing, Visualization, Writing – Original Draft, Project administration, Funding acquisition

Declaration of Competing Interest

The authors declare no conflict of interest.

References

CDC. Coronavirus Disease 2019 (COVID-19). Centers for Disease Control and Prevention. https://www.cdc.gov/coronavirus/2019-ncov/prevent-getting-sick/about-face-coverings.html. Published February 11, 2020. Accessed September 10, 2020.

Ogawa, S., Lee, T.M., Kay, A.R., Tank, D.W., 1990. Brain magnetic resonance imaging with contrast dependent on blood oxygenation. Proc. Natl. Acad. Sci USA 87, 9868–9872.

Davis, T.L., Kwong, K.K., Weisskoff, R.M., Rosen, B.R., 1998. Calibrated functional MRI: Mapping the dynamics of oxidative metabolism. Proc. Natl. Acad. Sci. USA 95, 1834–1839.

Kastrup, A., Li, T.Q., Glover, G.H., Moseley, M.E., 1999. Cerebral blood flow-related signal changes during breath-holding. AJNR Am. J. Neuroradiol. 20, 1233–1238.

Buxton, R.B., Frank, L.R., 1997. A model for the coupling between cerebral blood flow and oxygen metabolism during neural stimulation. J. Cereb. Blood Flow Metab. 17, 64–72. doi:10.1097/00004647-199701000-00009.

Wise, R.G., Pattinson, K.T.S., Bulte, D.P., et al., 2007. Dynamic forcing of end-tidal carbon dioxide and oxygen applied to functional magnetic resonance imaging. J. Cereb. Blood Flow Metab. 27, 1521–1532. doi:10.1038/sj.jcbfm.9600465.

Grubb, R.L., Raichle, M.E., Eichling, J.O., Ter-Pogossian, M.M., 1974. The effects of changes in PaCO2 on cerebral blood volume, blood flow, and vascular mean transit time. Stroke 5, 630–639. doi:10.1161/01.str.5.5.630.

Glover, G.H., 1999. Deconvolution of impulse response in event-related BOLD fMRI. Neuroimage 9, 416–429. doi:10.1006/nimg.1998.0419.

Warner, M.T., Patel, B., 2018. Mechanical Ventilation. In: Hagberg and Benumof's Airway Management. Elsevier, Philadelphia, PA, pp. 804–820 e4.

Glover, G.H., Law, C.S., 2001. Spiral-in/out BOLD fMRI for increased SNR and reduced susceptibility artifacts. Magn. Reson. Med. 46, 515–522.

Glover, G.H., Li, T.Q., Ress, D., 2000. Image-based method for retrospective correction of physiological motion effects in fMRI: RETROICOR. Magn. Reson. Med. 44, 162–167.

Chang, C., Cunningham, J.P., Glover, G.H., 2009. Influence of heart rate on the BOLD signal: the cardiac response function. NeuroImage 44. doi:10.1016/j.neuroimage.2008.09.029, 857–69.

Jenkinson, M., Beckmann, C.F., Behrens, T.E., Woolrich, M.W., Smith, S.M., 2012. FSL. NeuroImage 62. doi:10.1016/j.neuroimage.2011.09.015, 782–90.

Bharatendu, C., Ong, J.J.Y., Goh, Y., et al., 2020. Powered air purifying respirator (PAPR) restores the N95 face mask induced cerebral hemodynamic alterations among healthcare workers during COVID-19 Outbreak. J. Neurol. Sci. 417, 117078. doi:10.1016/j.jns.2020.117078.

Prisman, E., Slessarev, M., Han, J., et al., 2008. Comparison of the effects of independently-controlled end-tidal PCO$_2$ and PO$_2$ on blood oxygen level–dependent (BOLD) MRI. J. Magn. Resonance Imaging 27, 185–191. doi:10.1002/jmri.21102.

Voyvodic, J.T., 2006. Activation mapping as a percentage of local excitation: fMRI stability within scans, between scans and across field strengths. Magn Reson Imaging 24, 1249–1261. doi:10.1016/j.mri.2006.04.020.